

In presenting the dissertation as a partial fulfillment of the requirements for an advanced degree from the Georgia Institute of Technology, I agree that the Library of the Institution shall make it available for inspection and circulation in accordance with its regulations governing materials of this type.

I agree that permission to copy from, or to publish from, this dissertation may be granted by the professor under whose direction it was written, or, in his absence, by the dean of the Graduate Division when such copying or publication is solely for scholarly purposes and does not involve financial gain.

It is understood that any copying from, or publication of, this dissertation which involves potential financial gain will not be allowed without written permission.

A STUDY OF THE RESIDUAL LATERAL PRESSURES  
INDUCED IN A COHESIONLESS SOIL  
AFTER COMPACTION

A THESIS

Presented to  
the Faculty of the Graduate Division  
Georgia Institute of Technology

In Partial Fulfillment  
of the Requirements for the Degree  
Master of Science in Civil Engineering

By  
Charles Howell Mullis, Jr.

June 1956

12

A STUDY OF THE RESIDUAL LATERAL PRESSURES  
INDUCED IN A COHESIONLESS SOIL  
AFTER COMPACTION

Approved:

*[Handwritten signature]*

Date Approved by Chairman:

*5/30/50*

## ACKNOWLEDGEMENT

The writer wishes to express his appreciation to the many persons whose kind assistance made possible the undertaking of this project.

Especial thanks are extended to Professor George F. Sowers for his help in selection of the problem and his guidance throughout the investigation. Thanks are also due the other members of the thesis committee, Professor Don Jones and Dr. William Mullen.

## TABLE OF CONTENTS

	Page
ACKNOWLEDGEMENT . . . . .	ii
LIST OF TABLES . . . . .	iv
LIST OF ILLUSTRATIONS . . . . .	v
ABSTRACT . . . . .	vii
CHAPTER	
I. INTRODUCTION . . . . .	1
II. EQUIPMENT . . . . .	5
III. CALIBRATION OF EQUIPMENT . . . . .	12
IV. TEST PROCEDURE . . . . .	16
V. THEORY OF RESIDUAL LATERAL EARTH PRESSURES .	19
VI. ANALYSIS OF RESULTS . . . . .	22
VII. CONCLUSIONS AND RECOMMENDATIONS . . . . .	28
APPENDIX . . . . .	29
BIBLIOGRAPHY . . . . .	51

## LIST OF TABLES

Table	Page
1. Tabulation of the Different Values of Pressure .	27
2. Poisson's Ratio . . . . .	31
3. Test 1 - Dry-Tamped Soil . . . . .	40
4. Test 2 - Dry-Loose Soil . . . . .	42
5. Test 3 - Wet-Tamped Soil . . . . .	44
6. Test 4 - Wet-Loose Soil . . . . .	46
7. Test 5 - Flooded Soil . . . . .	48
8. Average Water Content and Average Density . . .	50

## LIST OF ILLUSTRATIONS

Figure	Page
1. Earth Pressure Cell Showing Leading Dimensions .	8
2. Schematic Wiring Diagram of the Cell and Indicator . . . . .	9
3. Opened Cell Showing Strain Gages and Closed Cell Sealed and Ready for Use . . . . .	15
4. Calibration Equipment, L. to R. Manometer, Calibration Cylinder, Switching Box, Strain Gage Indicator . . . . .	15
5. Test Pit Showing Pressure Cells in Place . . . . .	15
6. Close-up of Pressure Cell Mounted on Wall of Test Pit . . . . .	15
7. Test Pit Showing Location of Cells . . . . .	18
8. Lateral Pressures Resulting from Vertical Stresses . . . . .	19
9. Pressure-Depth Curve, Dry Sand . . . . .	25
10. Pressure-Depth Curve, Moist Sand . . . . .	25
11. Pressure-Depth Curve, Flooded Sand . . . . .	26
12. Grain Size Distributor of Sand . . . . .	30
13. Stress Strain Curve - Lateral Pressure Equals 1880 psf . . . . .	32
14. Stress Strain Curve - Lateral Pressure Equals 1220 psf . . . . .	33
15. Stress Strain Curve - Lateral Pressure Equals 600 psf . . . . .	33
16. Mohr's Circle - Angle of Internal Friction . . .	34
17. Mohr's Circle - Angle of Internal Friction . . .	34
18. Mohr's Circle - Angle of Internal Friction . . .	35
19. Calibration Curve - Cell No. 1 . . . . .	36

20.	Calibration Curve - Cell No. 2 . . . . .	37
21.	Calibration Curve - Cell No. 3 . . . . .	38
22.	Calibration Curve - Cell No. 4 . . . . .	39
23.	Pressure-Time - Test No. 1 . . . . .	41
24.	Pressure-Time - Test No. 2 . . . . .	43
25.	Pressure-Time - Test No. 3 . . . . .	45
26.	Pressure-Time - Test No. 4 . . . . .	47
27.	Pressure-Time - Test No. 5 . . . . .	49



## ABSTRACT

The pressure exerted by the earth on a structure has always been a problem confronting structural designers. The object of this thesis is to determine the magnitude of lateral pressures remaining after compaction of a cohesionless backfill was completed.

In the past studies have been made of many aspects of the problem of earth pressures. However, all these studies were limited to in-place soils or to soils that were, in essence, dumped into place.

It has long been known that compaction produces lateral pressures, but there is little information on the character or the magnitude of these pressures.

There are three common methods used to place a backfill.

Method 1. The soil is dumped in place without compaction.

Method 2. The soil is placed in layers and each layer or lift is compacted by some mechanical tamping device.

Method 3. The soil is suspended in water and pumped in place as a semi-fluid.

For this thesis a study of residual lateral pressures in compacted cohesionless soil was made, and the pressures induced by dumping the soil were used as a comparison. The

flooded case was also studied, since pressures in this type soil should lie somewhere between the values for tamped and loose soil. These tests were run with the soil both air-dry and moist.

The work on this thesis can logically be divided into four steps:

- a) Develop a device for measuring residual lateral pressures.
- b) Develop a method to calibrate this measuring device.
- c) Measure residual lateral pressures in the field, and study their variations with time.
- d) Compare the field measurements with an analytical solution.

The device that was used to measure pressures consisted of an aluminum frame 4 inches in diameter and  $1/2$  in. thick with a depression in the center. An aluminum diaphragm  $1/16$  in. thick and of the same diameter was secured to the frame. SR-4 strain gages were used to measure the deflection of this diaphragm caused by the earth pressures. This cell was calibrated by air pressure.

Five field tests were run. The tests were moist and dry tamped soil, moist and dry loose soil and flooded soil.

A theoretical analysis of the problem shows that the maximum residual lateral pressure can be as much as 1.44 times the vertical soil pressure.

Results of the test indicate:

- a) The calibration of the cells is consistent with time.
- b) The magnitude of residual lateral pressures will be between the neutral and theoretical residual lateral pressure.
- c) The magnitude of residual pressures will not vary with time.
- d) Residual lateral pressures will be larger than lateral pressures of loose soil.

## CHAPTER I

### INTRODUCTION

General Background. The pressure exerted by the earth on a structure has always been a problem confronting structural designers.

In the past studies have been made of many aspects of the problem of earth pressures. Coulomb (1) in 1776 developed a purely theoretical study of pressures behind a retaining wall. In his studies he assumed that the wall leans outward from the soil as pressure is applied and that a plane of shear failure occurs. Rankine (5) studied the state of stress within a loose granular mass. His analysis was based on the assumption that the slightest deformation of the soil is sufficient to bring into play its full frictional resistance and immediately to produce an "active state" if the soil tends to expand parallel to its surface, and a "passive" state if it tends to compress parallel to its surface. Résal (7) attempted to expand Rankine's work to include cohesive soils.

Terzaghi (12) pointed out that "The fundamental assumptions of Rankine's earth pressure theory are incompatible with the known relation between stress and strain in soils, including sand. Therefore the use of this theory should be discontinued."

It can be noted that all of these studies were limited to in-place soils or to soils that were, in essence, dumped into place.

Experience shows that when a structure is built on an in-place soil or a dumped loose soil, excess settlement will occur. This settlement will cause the structure to crack or completely fail. Further, experience has shown that if the soil is compacted sufficiently, that will prevent excess settlement.

It has long been known that compaction produces lateral pressures, but there is little information on the character or the magnitude of these pressures.

When a soil is compacted, the total depth of the soil is reduced. This reduced depth is compensated by a lateral bulging of the soil so that the unit volume remains the same. This lateral bulge, pushing against an adjacent object, whether it be soil or a structure, is what causes lateral pressure.

If the adjacent object does not move during the time this pressure is being exerted, neutral earth pressure is established. The value of neutral earth pressure is expressed by

$$\sigma_3 = \frac{\mu}{1-\mu} \sigma_1 \quad \text{where} \quad (\text{Eq. 1})$$

$\sigma_3$  = the lateral earth pressure,

$\sigma_1$  = the vertical earth pressure, and

$\mu$  = Poisson's ratio for the particular soil. The expression  $\frac{\mu}{1-\mu}$  is called the coefficient of neutral earth



pressure and is sometimes expressed  $K_0$ .

If the adjacent object can move away from the bulging soil until the bulging soil is just able to continue making contact, active earth pressure is said to be established. The value of the active earth pressure may be expressed for a cohesionless soil as

$$\sigma_3 = \sigma_1 \tan^2 (45^\circ - \frac{\phi}{2}) \text{ where} \quad (\text{Eq. 2})$$

$\sigma_3$  = the active earth pressure,

$\sigma_1$  = the vertical pressure and

$\phi$  = the angle of internal friction for the particular soil.

$\tan^2 (45^\circ - \frac{\phi}{2})$  is the coefficient of active earth pressure,  $K_a$ .

Terzaghi (11) (13), Spangler (8) (9) (10) and Tschebotarioff (14) among others have investigated lateral earth pressures against retaining walls caused by superimposing loads at the surface. The cases of both the yielding and non-yielding wall were studied. In all the above tests, no study was made of residual lateral pressures which remained after the superimposed load was removed.

The object of this thesis is to determine the magnitude of lateral pressures remaining after compaction of a cohesionless backfill was completed.

There are three common methods used to place a backfill.

Method 1. The soil is placed in layers and each layer

or lift is compacted by some mechanical tamping device.

Method 2. The soil is dumped in place without compaction.

Method 3. The soil is suspended in water and pumped in place as a semi-fluid.

For this thesis a study of residual lateral pressures in compacted cohesionless soil was made, and the pressures induced in this type soil should lie somewhere between the values for tamped and loose soil.

An additional variable was studied in the case of the tamped and the loose soils. Tests were made with the soil air dry and with the soil containing enough moisture to insure the development of capillary tension.

The effect of time on the residual pressures was also studied as an additional variable.

The work on this thesis can logically be divided into four steps:

- a) Develop a device for measuring residual lateral pressures.
- b) Develop a method to calibrate this measuring device.
- c) Measure residual lateral pressures in the field, and study their variations with time.
- d) Compare the field measurements with an analytical solution.

The following chapters of this thesis show how these four steps were carried out.

## CHAPTER II

### EQUIPMENT

There have been many attempts to develop a device for measuring lateral pressures in soil.

A system adopted by Spangler (10) measured the force required to release a steel band from confinement in the soil. Then by correlating this force with the friction of the soil on the band, an approximation of the lateral pressure could be obtained.

There were also attempts to develop an earth pressure cell. The basic component of most earth pressure cells is a diaphragm that deflects when subjected to earth pressure. The main problem with any cell is correlating the pressure and the resulting deflection. Goldbeck (2) developed a cell that met with some success. Goldbeck measured the external pressure by balancing it with air pressure within the cell. A cell was developed in England that utilized a varying sound pitch resulting from varying tension on a thin wire attached to a diaphragm.

The development of the electrical resistivity strain gage offered another means of evaluating the deflection in a cell diaphragm. The electrical resistivity strain gage utilizes the principle that the resistance to a flow of electrical current is inversely proportional to the cross-



sectional area of the conducting wire.

The SR-4 strain gage consists of a thin wire mounted on a very thin piece of paper. A felt covering is glued on top to protect the wire. The gage is attached to the object to be tested by glueing the gage to the object. After the gage is firmly mounted, any movement in the object will in turn cause the wire to increase or decrease in area. The amount of resistance change in the gage is measured by the strain gage indicator. This indicator utilizes the principle of the Wheatstone bridge in measuring resistance, and the indicator is calibrated to read directly in micro-inches per inch of strain.

The Waterways Experiment Station of the Corps of Engineers at Vicksburg, Mississippi (17), was an early user of the strain gage in developing a cell used to measure earth pressures in large earth dams. Their cell was very carefully designed either to eliminate or to measure the variables in earth pressures. Because of this careful design, the cell costs between \$300 and \$500 and is used for long-term measurements.

It was decided to use SR-4 strain gages in the earth pressure cells to measure residual lateral pressures in tests conducted in this thesis work.

The cell that was used consisted of an aluminum frame 4 inches in diameter and  $1/2$  inch thick with a depression in the center. An aluminum diaphragm  $1/16$  inch thick and of the

same diameter was secured to the frame by 12 machine screws. The measuring, or active, gage was cemented to the diaphragm and the temperature compensating, or dummy, gage was attached to the frame. The two gages were connected internally by a common lead so that only three leads were needed. Tapped lead holes were drilled in the frame. Fig. 1 shows a drawing of the cell and Fig. 2 shows a schematic wiring diagram of the cell and indicator. Gasket compound was used to seal the diaphragm to the frame, and beeswax was used to coat the gages and seal the access holes. Before sealing, the felt covers were removed from both gages to give more room for lead wires inside the cell.

Before any cell can be used for field measurements it must be calibrated. The calibration equipment used consisted of a steel cylinder 11 inches in diameter and 12 inches high. A concrete block was placed inside to represent a retaining wall. The cell was placed on this wall and the remainder of the cylinder was filled with sand. An access hole was provided in the side of the cylinder for the lead wires. A thin rubber membrane was placed over the sand and a steel top equipped with the necessary fittings was bolted to the cylinder. Compressed air was introduced between the top and the membrane to produce the necessary pressure. It was felt that compressed air acting on a rubber membrane would closely approximate the uniform pressure experienced in a soil mass. A mercury manometer was placed between the air supply and the

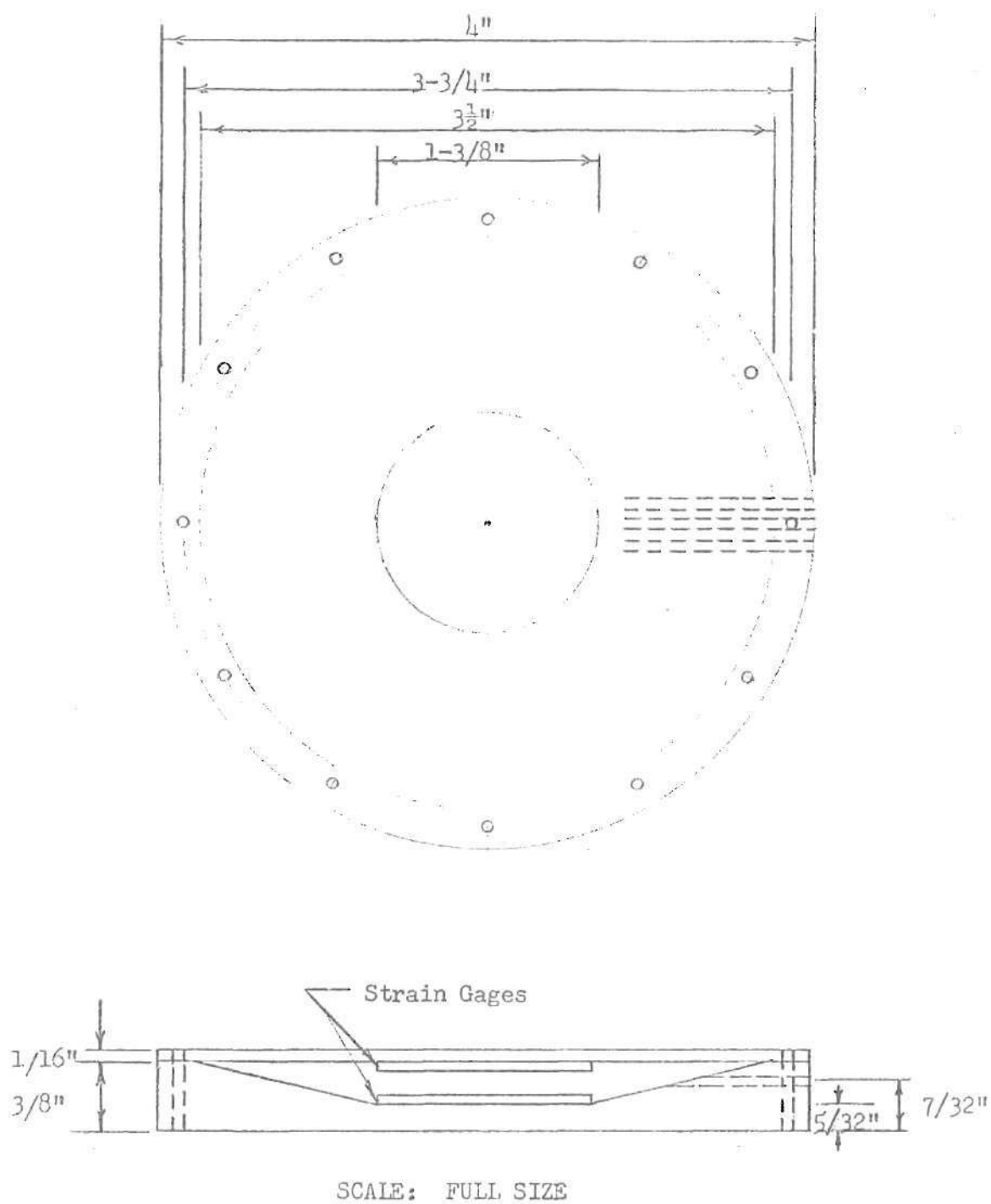


Fig. 1. Earth Pressure Cell Showing Leading Dimensions

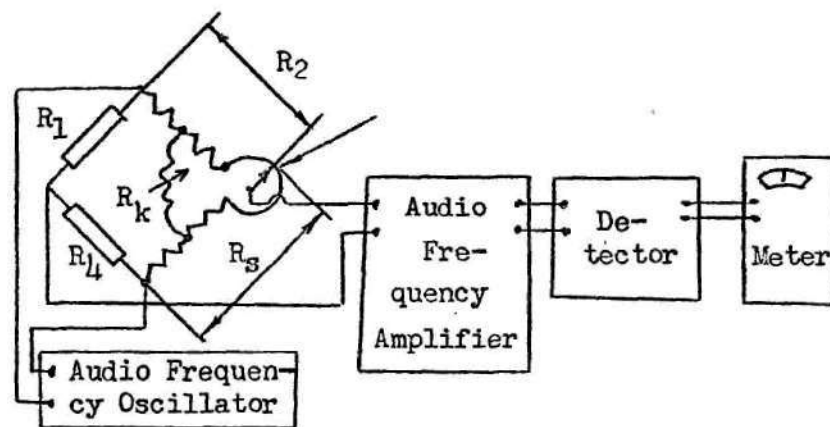


Fig. 2. Schematic Wiring Diagram of The Cell and Indicator

cylinder to measure the air pressure. This manometer was calibrated to read directly in pounds per square foot (psf), and a needle valve was supplied to allow close control of the air pressure.

A Baldwin Type L strain indicator was used to measure the strains.

A Baldwin six position switching box was used to allow instantaneous switching from one cell to another. This prevented any error caused by changing leads.

Standard laboratory equipment was used to determine the physical characteristics of the sand used. This consisted of a standard tri-axial shear device used to get the values of strain with stress and to determine the value  $\phi$ , the angle of internal friction of the sand. U. S. Standard sieves were used to obtain the grain size and distribution. A microscope was used to determine the grain shape. Flasks and an analytical balance were used to determine the specific gravity of solids.

The device used to determine Poisson's ratio was developed by Robb (6) and others at the Georgia Institute of Technology. It is a steel cylinder with horizontal slots sawed halfway around. Strain gages were mounted on the cylinder, and when a vertical load was placed on the sand the corresponding lateral strain could be read. By use of calibration charts, the value of Poisson's ratio,  $\mu$ , could be determined.

The test pit used was twelve feet long, four feet wide,

and five feet deep at the test end. The other end was three feet deep. The pit was lined with concrete to give a water-tight lining. Six inches of pea gravel was placed in the bottom to aid in drainage.

The sand used was a natural river sand obtained from the Chattahoochee River near Atlanta, Georgia. The sand was sub-angular in shape and uniformly graded. The specific gravity of solids was 2.64.

See Appendix for results of the above tests.



### CHAPTER III

#### CALIBRATION OF EQUIPMENT

The cell was placed on the concrete block in the cylinder and the remaining space was filled with sand. The rubber membrane was placed over the sand and the steel top was then bolted in place.

Air pressure was then introduced between the top and the membrane.

The magnitude of pressure was read from a mercury manometer calibrated directly in pounds per square foot (psf).

The cylinder was loaded in 100 psf increments to 500 psf. Readings were taken of the strain produced by each increment of loading. At 500 psf, the loading increment was increased to 500 psf, and loading was continued to a maximum value of 4000 psf. The unloading schedule was the reverse of the loading schedule.

During the preliminary trials several facts became apparent which had to be taken into account in future tests.

- a) The calibration curve was not linear.
- b) The unloading curve was not coincident with the loading curve.
- c) Each cell had a unique calibration curve.

- d) Each cell had to be "worked out" by cycling about 25 times before the calibrations became constant.
- e) The type soil affected the shape of the curve.
- f) The zero reading of the indicator changed with time.

Each cell was calibrated independently using sand from the field test.

Perry and Lissner (4) suggest a method of eliminating zero drift with time. A reading is taken with the active and dummy gages in their normal position in the Wheatstone bridge. Then the positions of the two gages are reversed in the bridge and a new reading is taken. The average of the two readings will give the zero value for that particular reading.

By cross-connecting two positions on the switching box, this reversal of positions of the active and dummy gages could be accomplished merely by changing from one switch position to another.

Before each cell was calibrated, it was load-cycled about 25 times. This cycling effect stabilized the cell readings. Apparently plastic flow of the gasket material occurred during cycling and there was a repositioning of the diaphragm.

After each cell had stabilized, usually about three runs gave enough points to define a smooth loading and unloading curve.



A recalibration of the cells indicated that the calibration curves did not change with time during the period of these tests.

Fig. 4 shows the calibration equipment setup. The calibration curves for the four cells used may be found in the Appendix.

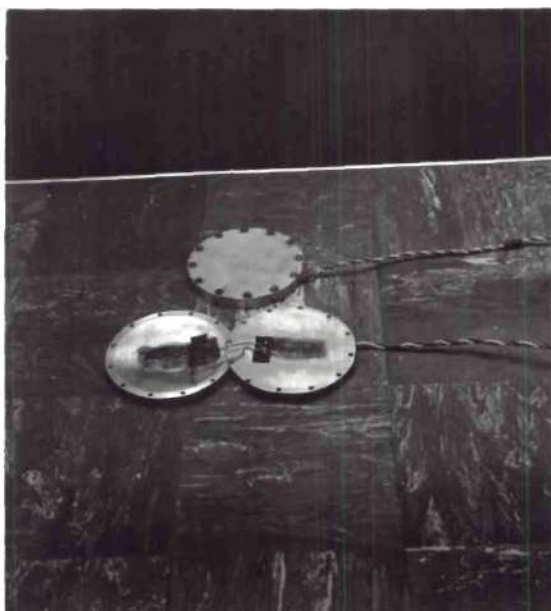


Fig. 3. Opened Cell Showing Strain Gages and Closed Cell Sealed and Ready for Use

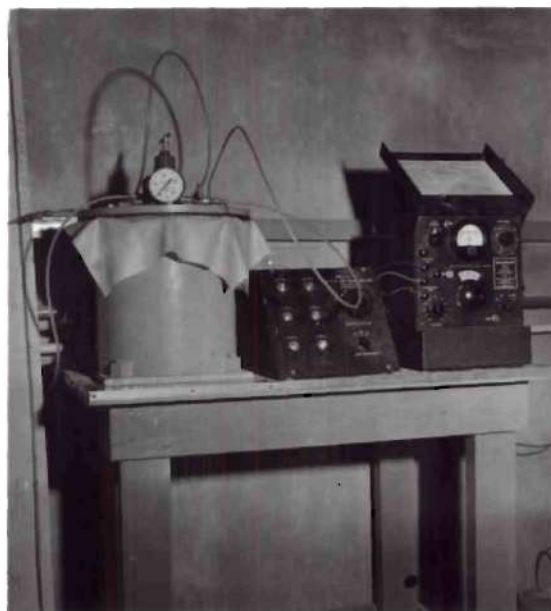


Fig. 4. Calibration Equipment, L. to R. Manometer, Calibration Cylinder, Switching Box, Strain Gage Indicator

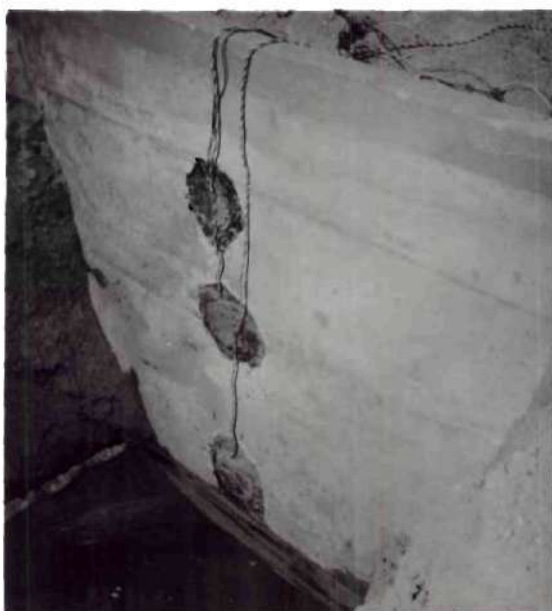


Fig. 5. Test Pit Showing Pressure Cells in Place

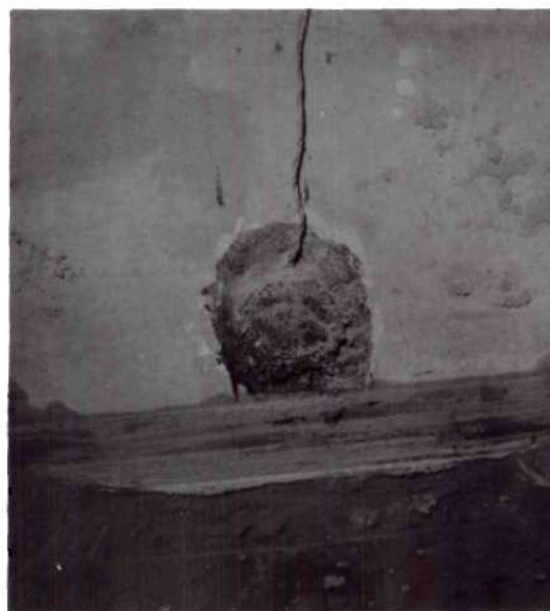


Fig. 6. Close-up of Pressure Cell Mounted on Wall of Test Pit

## CHAPTER IV

### TEST PROCEDURE

In Chapter I it was pointed out that there are three common methods of backfilling. In running these tests the control values would be those of the loose soil. The values of residual lateral pressures obtained after tamping the dry and moist sands, can then be compared to the pressures in the loose sand. The pressures in the soil after flooding will also be compared, since the density of the soil would be between that of loose sand and that of a compacted sand.

Three cells were mounted against the face of one wall in the test pit as shown in Fig. 5. Plaster of Paris was used as the bonding agent.

Test I. This test was of the dry tamped sand. The sand was placed in four-inch lifts and compacted with a pneumatic tamper. Both direct and reverse strain readings were taken at frequent intervals during the filling process.

After the pit was filled, readings were continued at regular intervals until a definite trend of residual strains could be detected.

Test II. This test run was that of dry sand in a loose state. The sand was backfilled into the pit and readings taken as previously described.

Test III. Before this test was run, the sand was mois-

tened until there was obvious capillary tension. The test was then run using the procedure of Test I.

While the test was in progress, the bottom cell exhibited evidence of grounding, and balancing the bridge became an impossibility. There is some evidence that the middle cell became grounded, but the instability of the bridge was not apparent during the test run.

Test IV. Before the start of the fourth test, all cells were dried and resealed. The test was of moist sand in the loose condition and was conducted in the same manner as Test II. About nine hours after the pit was backfilled, the cells started to exhibit instability again. Two hours of observations during this instability period led to the decision to terminate this phase of the test.

Prior to the fifth phase of the field test all cells were again dried and then painted with RC-0 asphalt in an attempt to waterproof them.

Test V. This test was run by jetting water into the soil as it was placed in the pit. After all of the soil had been placed water was added until ponding occurred in surface depressions. Even though the cells were in effect immersed in water during the duration of the test, there was no indication of shorting or grounding during the entire test period.

At the end of each test run, undisturbed samples were taken at approximately one foot depth increments for purposes of determining the density of the soil. At the same time

samples were taken to determine the water content of the sand.

The Appendix contains tables of the test data, and graphs of pressure plotted against time for each test run.

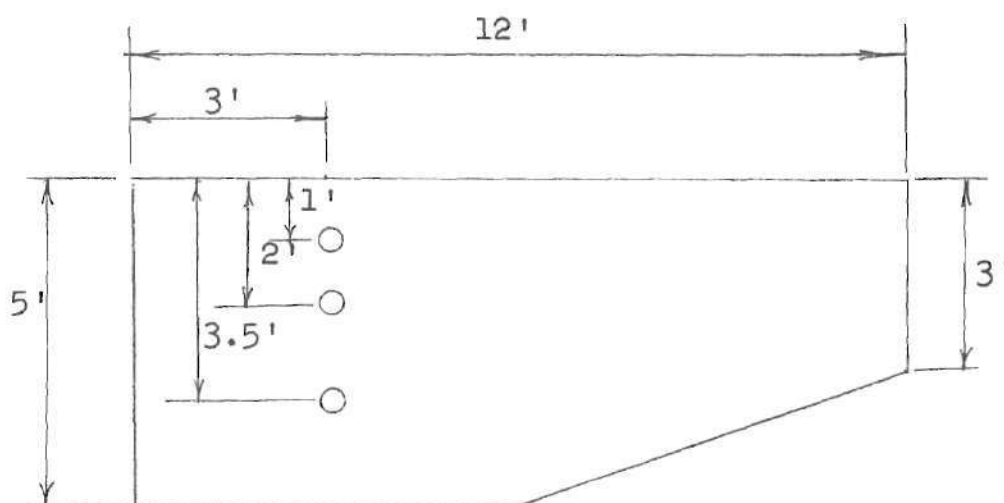


Fig. 7 - Test Pit Showing Location  
of Pressure Cells

## CHAPTER V

## THEORY OF RESIDUAL LATERAL EARTH PRESSURES

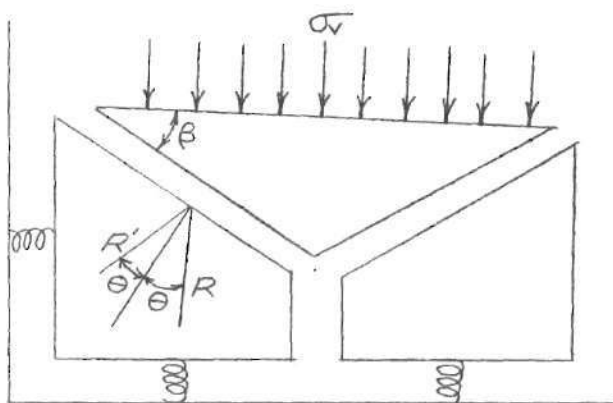


FIG. 8

In Fig. 8 let the two trapezoidal blocks of earth be acted upon by the wedge-shaped block, which in turn is acted upon by an external pressure,  $\sigma_v$ . When the wedge-shaped block moves down vertically it is deflected some angle  $\beta$ . Experience has shown that, for a cohesionless soil, this angle is about  $60^\circ$ . The trapezoidal blocks can be thought of as supported by springs. When the wedge acts on them, they are forced down and out. The downward force of the wedge is resisted by a reaction,  $R$ , which is offset by some angle,  $\Theta$ , from the normal to the plane of contact. The maximum value of  $\Theta$  would occur when the friction between the two blocks was greatest. That would be the instant before one block



slid against the other. When the external pressure is released, the wedge would attempt to return to its normal position due to the inherent elasticity of the particles. After the load has been released, R will swing to the other side of the normal line, and the angle it makes with the normal will again be the angle  $\Theta$ . The range of  $\Theta$  will be from  $0^\circ$  to  $\Theta$  maximum just as motion impends. This will be equally true for  $\Theta$  on either side of the normal. The resultant after the load is released is  $R'$ .

Assume that the dimensions of the wedge are one unit wide on each side. Then the vertical force,  $F_v = \sigma_v \times 1$ , and the horizontal component of the reaction,

$$R_H = \frac{\sigma_v}{2} \times 1 \times \tan(\beta - \Theta).$$

The area acted upon is  $1 \times \tan\beta \times 1/2$ .

Therefore

$$\sigma_H = \sigma_v \frac{\tan(\beta - \Theta)}{\tan\beta}, \text{ and}$$

$$\frac{\sigma_H}{\sigma_v} = \frac{\tan(\beta - \Theta)}{\tan\beta}. \quad (\text{Eq. 3})$$

Proof of the relationship,

$$\frac{\sigma_H}{\sigma_v} = \frac{\mu}{1 - \mu}, \text{ where } \mu \text{ is Poisson's ratio, can be}$$

found in any standard textbook on soil mechanics.

The experimental value of  $\mu$  for the sand used for these tests was 0.424.

Thus

$$\frac{\sigma_H}{\sigma_v} = \frac{0.424}{0.576} = 0.735.$$

Introduction of this value into (Eq. 3) permits a solution of  $\Theta$ .

$$0.735 = \frac{\tan(\beta - \Theta)}{\tan \beta}, \text{ and } \beta = 60^\circ.$$

$$0.735 \times 1.73 = \tan(60^\circ - \Theta).$$

$$51.8^\circ = 60^\circ - \Theta.$$

Therefore

$$\Theta = 8.2^\circ.$$

At the residual condition,

$$\frac{\sigma_H}{\sigma_V} = \frac{\tan(\beta + \Theta)}{\tan \beta}. \quad (\text{Eq. 4})$$

For the maximum value of  $\Theta$ ,  $8.2^\circ$ ,

$$\frac{\sigma_H}{\sigma_V} = \frac{\tan(60^\circ + 8.2^\circ)}{\tan 60^\circ} = \frac{2.5}{1.73} = 1.44, \text{ and}$$

$$\sigma_{H_{\max}} = 1.44 \sigma_V. \quad (\text{Eq. 5})$$

Therefore the residual lateral pressure can be 1.44 times the vertical pressure, where the vertical pressure is equal to the weight of the soil above the plane of contact, and

$$\sigma_V = \gamma Z, \text{ where} \quad (\text{Eq. 6})$$

$\gamma$  = the unit weight of the soil and

$Z$  = the depth below the surface.



## CHAPTER VI

### ANALYSIS OF RESULTS

An examination of Figs. 9, 10 and 11 shows that the trend of residual lateral pressures measured in the field tests are in fair agreement with the theoretical lateral pressures. In all cases the measured values were somewhat less than the theoretical values.

Inspection of the test data shows that during the filling of the pit, large strains were experienced in cells that were as yet uncovered. It is suspected that these strains were caused by movement in the wall during the filling process.

Since the theoretical analysis was developed for a non-yielding wall, if the wall did move during the test, then the measured values would be less than the theoretical values. This was found to be the case in all tests.

Values of active and neutral lateral earth pressures are also shown in Figs. 9, 10 and 11.

In the tests conducted on dry sand, the measured values of residual lateral earth pressure in the top and middle cell agree with the values of the active pressure and the measured pressure in the bottom cell agrees with the value for neutral earth pressure. The wall apparently yielded from a depth of approximately three feet to the surface. Even though an

attempt was made to have the sand air dry for this test, there was some moisture present. This moisture would create capillary tension which would relieve some of the residual lateral pressure. It is felt that this is what happened in this test.

In the tests conducted on moist sand, the measured pressure on the top cell was found to lie between the neutral pressure and the theoretical. The measured pressure on the middle cell coincided with the active pressure at that depth.

While this test was being conducted, the bottom cell shorted out. However a good trend of pressures had been extrapolated to the end of the test. The extrapolated residual lateral pressure was found to lie between the neutral pressure and the theoretical pressure.

In the flooded test it was found that in all cases the measured pressures were less than the active earth pressure. This is contrary to theory, since the active earth pressure is the theoretical minimum pressure that can be experienced. The author can offer no explanation for this phenomenon.

In several tests, the pressures measured by the middle cell were less than those measured by the top cell. One explanation for this occurrence is that a weak spot developed in the soil behind the wall, and the wall was able to move out more in the vicinity of the middle cell than elsewhere.

Another possibility is that the wall is not of constant thickness. If the wall were thinner in the vicinity of the middle cell, then it could possibly deflect more, causing a reduced pressure at the middle cell.

Immediately after the compaction was terminated for each test, there was a large reduction in the magnitude of lateral pressures. The lateral pressure remaining was the residual lateral pressure and its magnitude did not change to any extent with time.

During the test made to determine Poisson's ratio for this sand, an auxiliary test was run to measure the residual lateral pressures in the sand. The values of residual lateral pressures determined in this manner were found to be slightly smaller than the pressures measured in the field tests.

The value of  $K_0$  determined by Robb's (6) apparatus was 0.735. This was higher than values obtained by Mazanti (3) and others using similar sand. However, their tests were run at much higher vertical pressures.

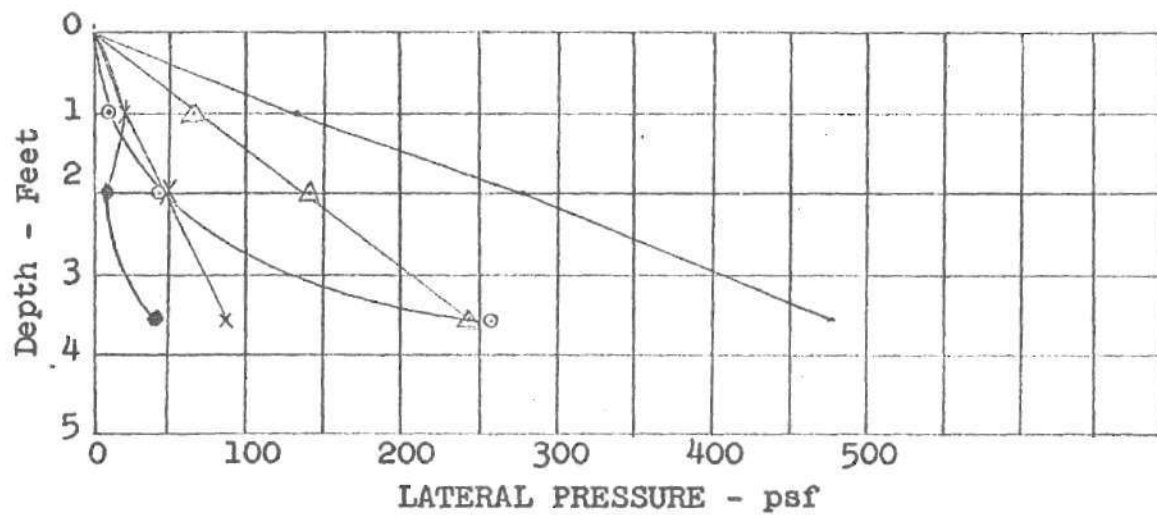


Fig. 9. Pressure-Depth Curve - Dry Sand

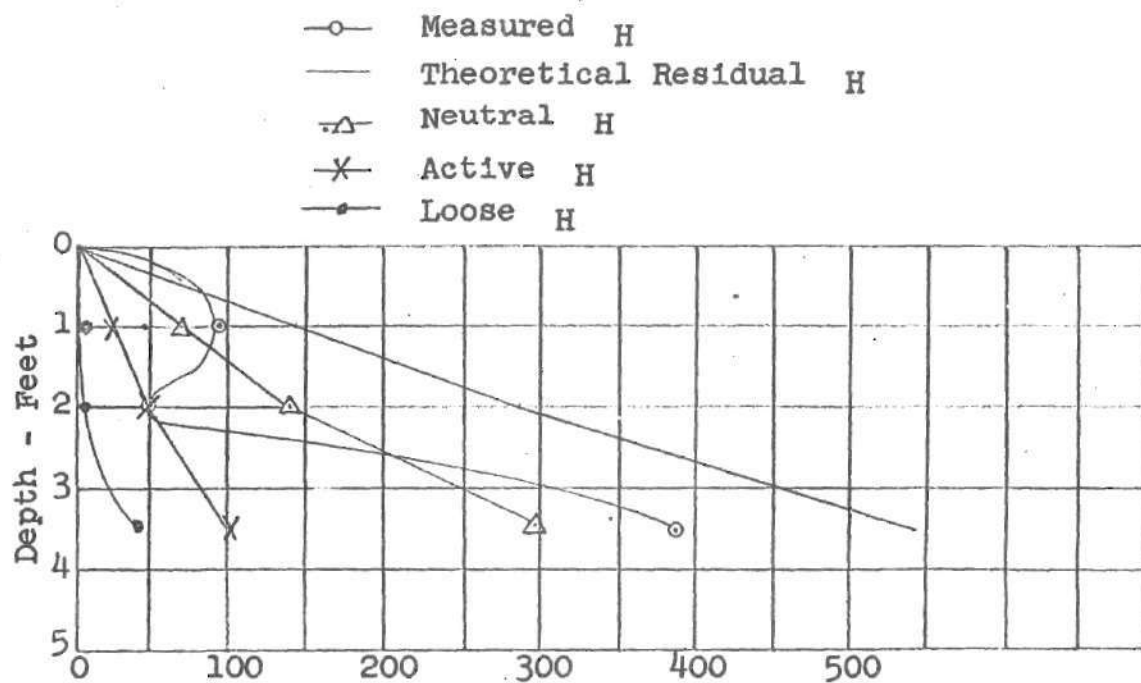


Fig. 10. Pressure-Depth Curve - Moist Sand

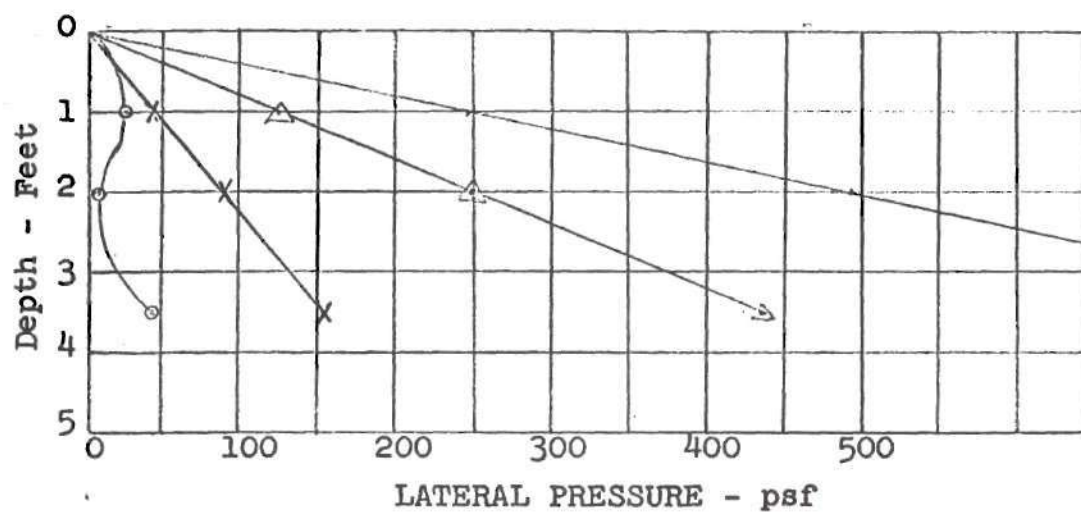


Fig. 11. Pressure-Depth Curve - Flooded Sand

- Measured H
- △— Neutral H
- ×— Active H
- Theoretical Residual H

Table 1. Tabulation of the Different Values of Pressure

## Dry Sand

Cell	Average Residual $\sigma_H$	Theoretical Residual $\sigma_H$	$\sigma_v = \gamma Z$	Neutral $\sigma_H = .735\sigma_v$	Active $\sigma_H = .26\sigma_v$	Loose Average $\sigma_H$
Top	15	131	91.1	67	23.6	24
Middle	45	275	191.4	140.8	50.5	11
Bottom	255	478	332	244	86.2	46

## Moist Sand

Top	95	141	97.6	71.7	25.4	6
Middle	50	278	193	141.8	50.1	5
Bottom	—	540	406	298	105.5	41

## Flooded

Top	28	245	170	125	44	
Middle	10	488	339	249	88	
Bottom	45	853	593	436	154	



## CHAPTER VII

### CONCLUSIONS AND RECOMMENDATIONS

The following significant conclusions were obtained from the results of this test.

- a) The calibration of the cells is consistent with time.
- b) The magnitude of residual lateral pressures will be between the neutral lateral pressure and the theoretical residual lateral pressure.
- c) The magnitude of residual lateral pressure will not vary with time.
- d) Residual lateral pressures remaining after compaction will be larger than lateral pressures of loose soil.

It is recommended that tests be made on many different types of sand to determine whether the type soil tested has any effect on the magnitude of residual lateral pressures.

An attempt should be made to improve the design of the cell without increasing the cost of the cell too much. A possibility would be to reduce the thickness of the diaphragm. This would in turn increase the sensitivity of the cell.

## APPENDIX



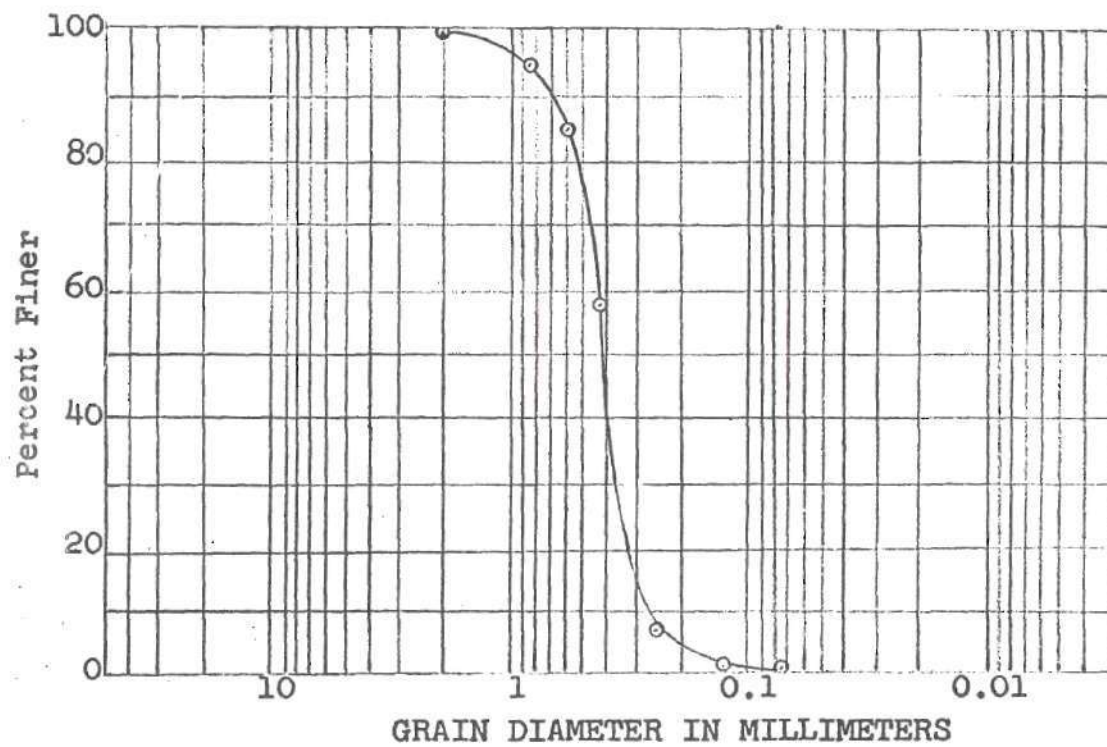


Fig. 12. Grain Size Distribution of Sand

Table 2. Poisson's Ratio

$\sigma_1$ psf	Active Strain $\mu$ in/in	$\epsilon_x \cdot .854$ $= \sigma_3$ psi	$\sigma_3$ psf	$\frac{\sigma_3}{\sigma_1} = K_0$	$\mu$	Residual $\sigma_3$
500	4	3.42	492	0.985	0.496	123
1000	6	5.13	738	.738	.424	123
1250	7	5.97	860	.688	.408	246
1500	8	6.83	983	.655	.395	492
1750	10	8.54	1230	.703	.412	615
2000	12	10.2	1470	.735	.423	615
2250	15	12.8	1833	.815	.449	615
2500	16	13.7	1972	.790	.441	615
2750	17	14.0	2020	.735	.423	615
3000	18	15.4	2220	.740	.425	615
3500	19	16.2	2330	.666	.400	738
4000	21	17.9	2580	.654	.392	738

Average  $\mu = 0.424$ Average  $K_0 = 0.735$

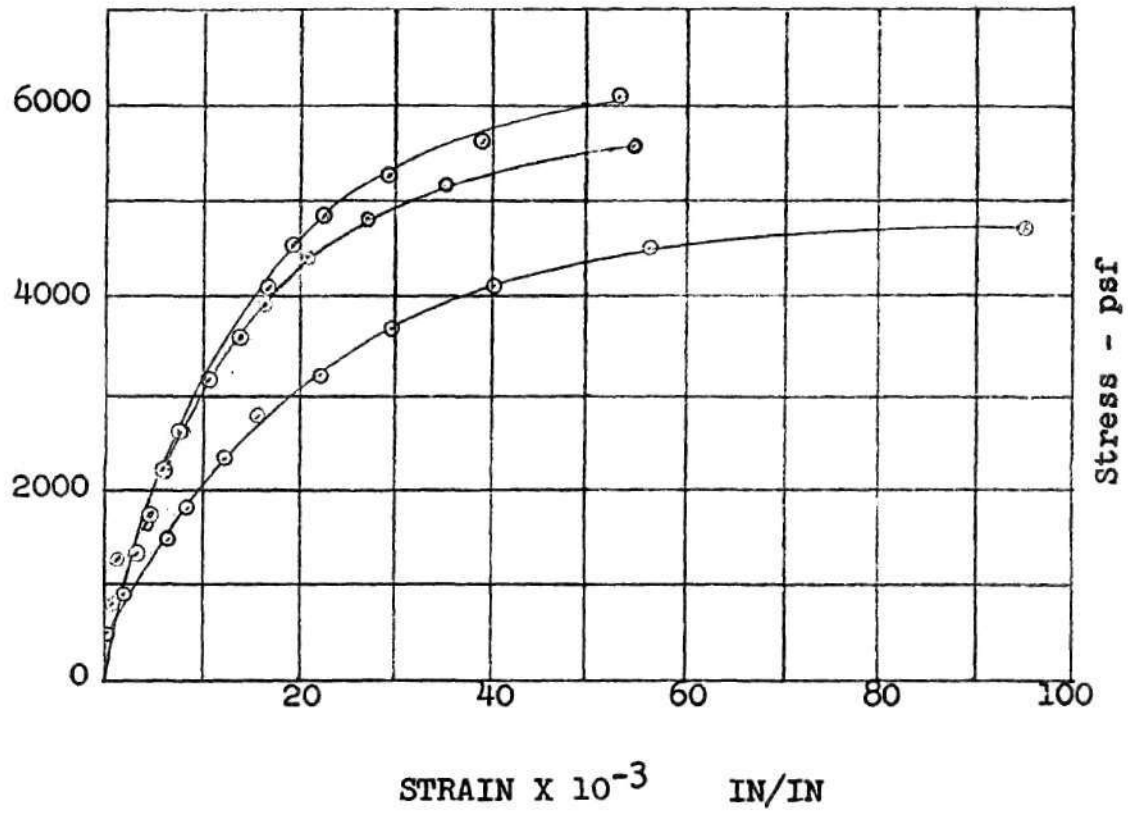


Fig. 13. Stress Strain Curve -  
Lateral Pressure Equals  
1880 psf - Tri - axial Shear

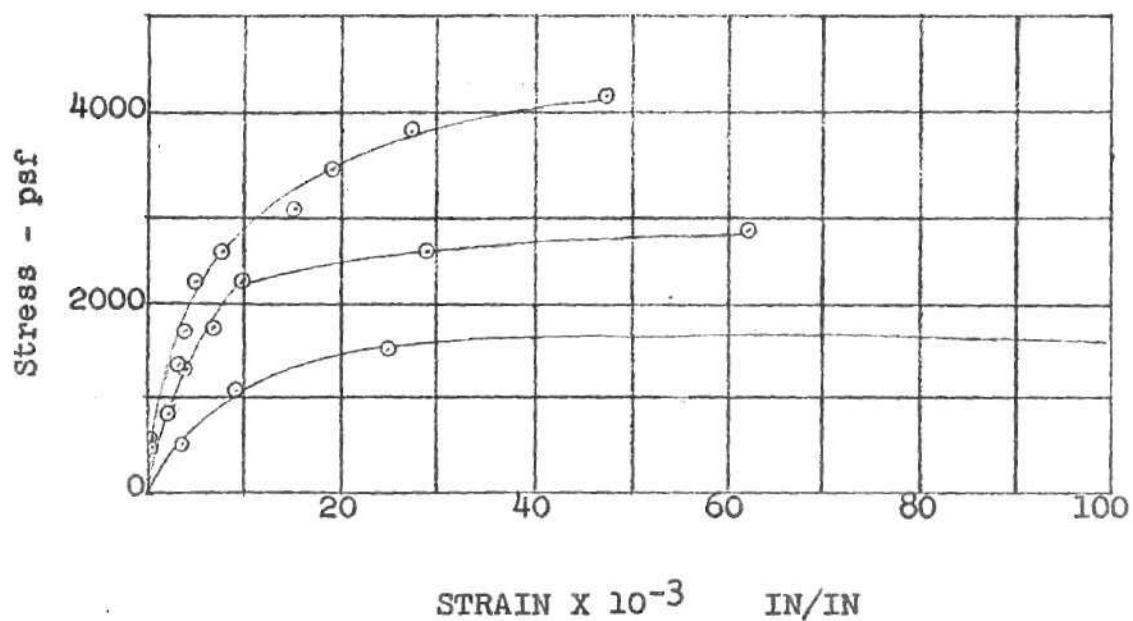


Fig. 14. Stress Strain Curve - Lateral Pressure Equals 1220 psf - Tri - axial Shear

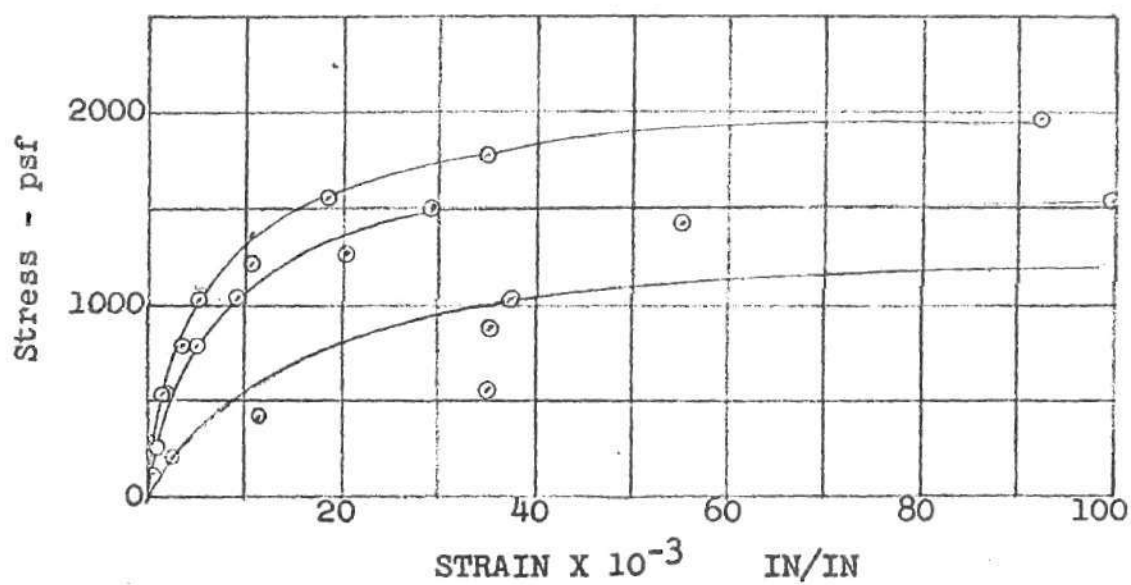


Fig. 15. Stress Strain Curve - Lateral Pressure Equals 600 psf

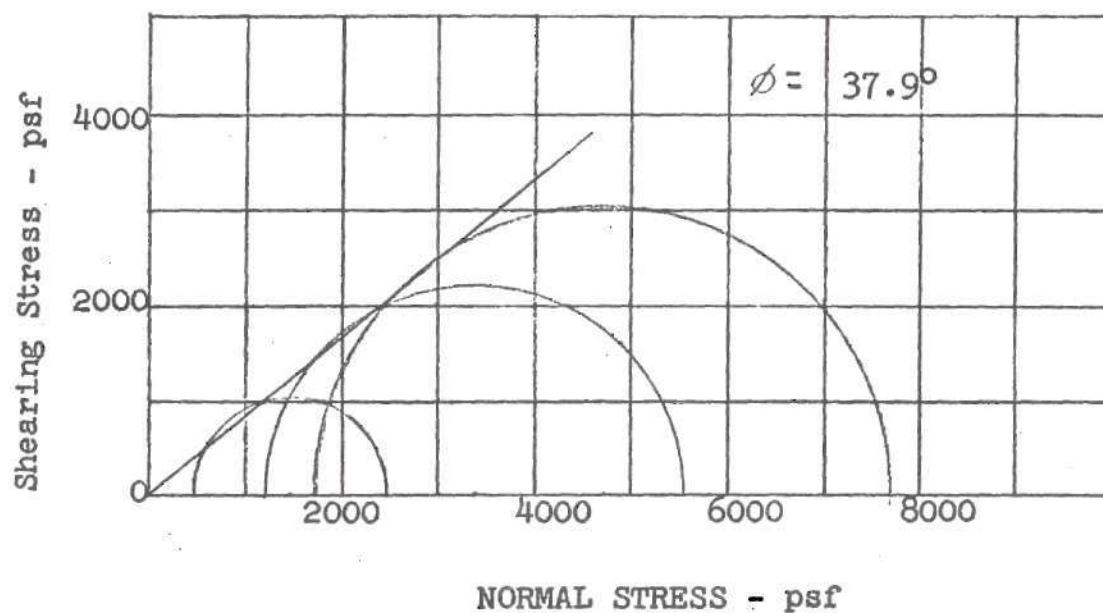


Fig. 16. Mohr's Circle - Angle of Internal Friction

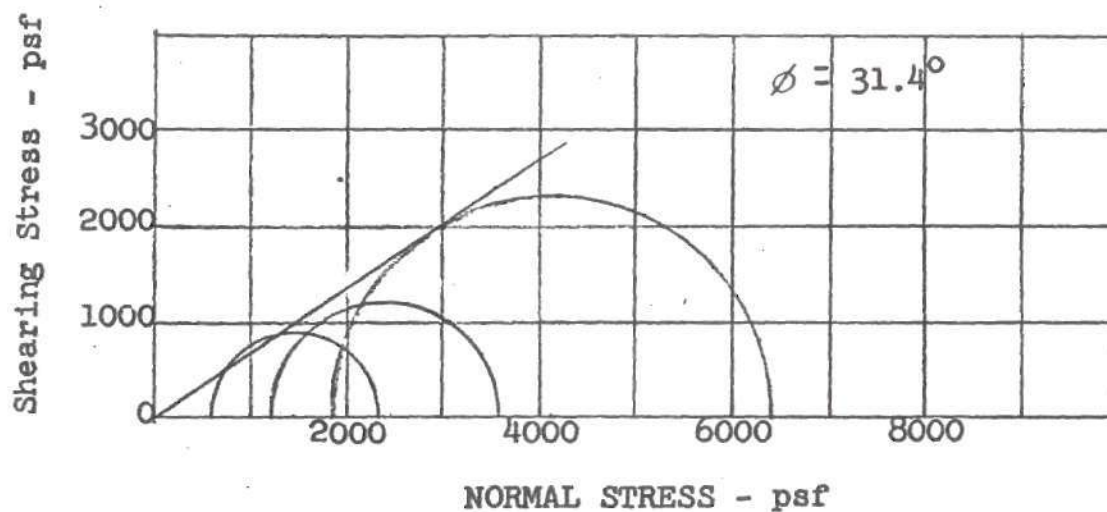


Fig. 17. Mohr's Circle - Angle of Internal Friction

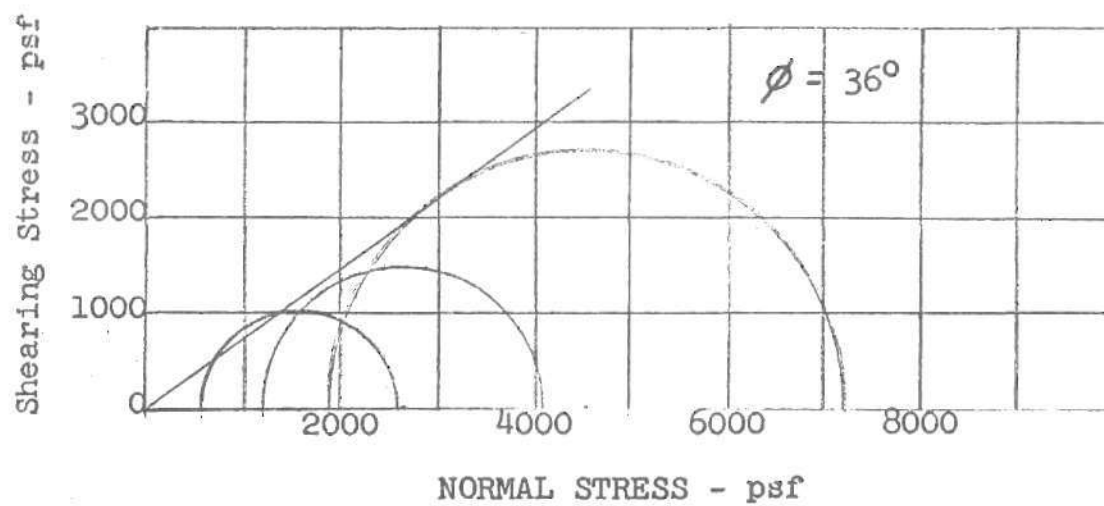


Fig. 18. Mohr's Circle - Angle of Internal Friction



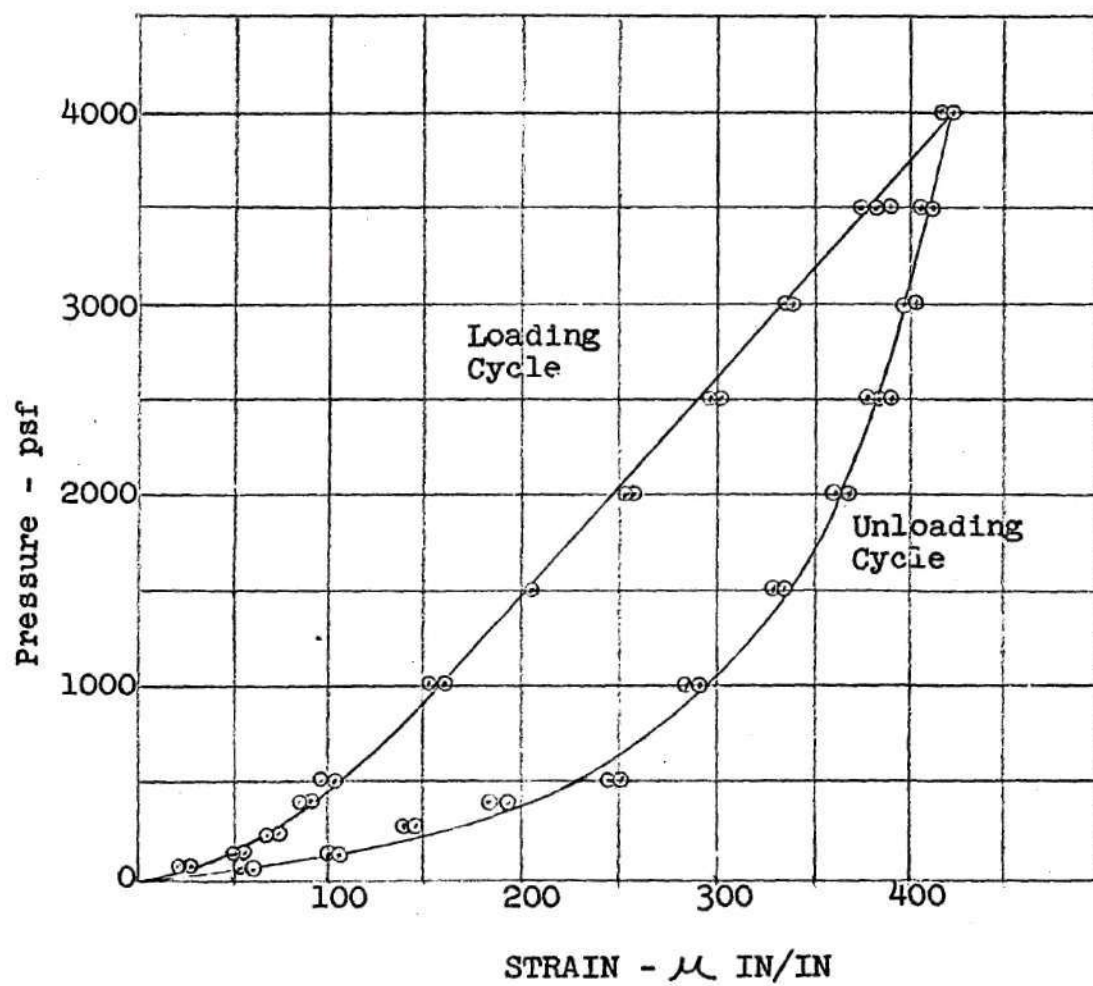


Fig. 19. Calibration Curve -  
Cell No. 1

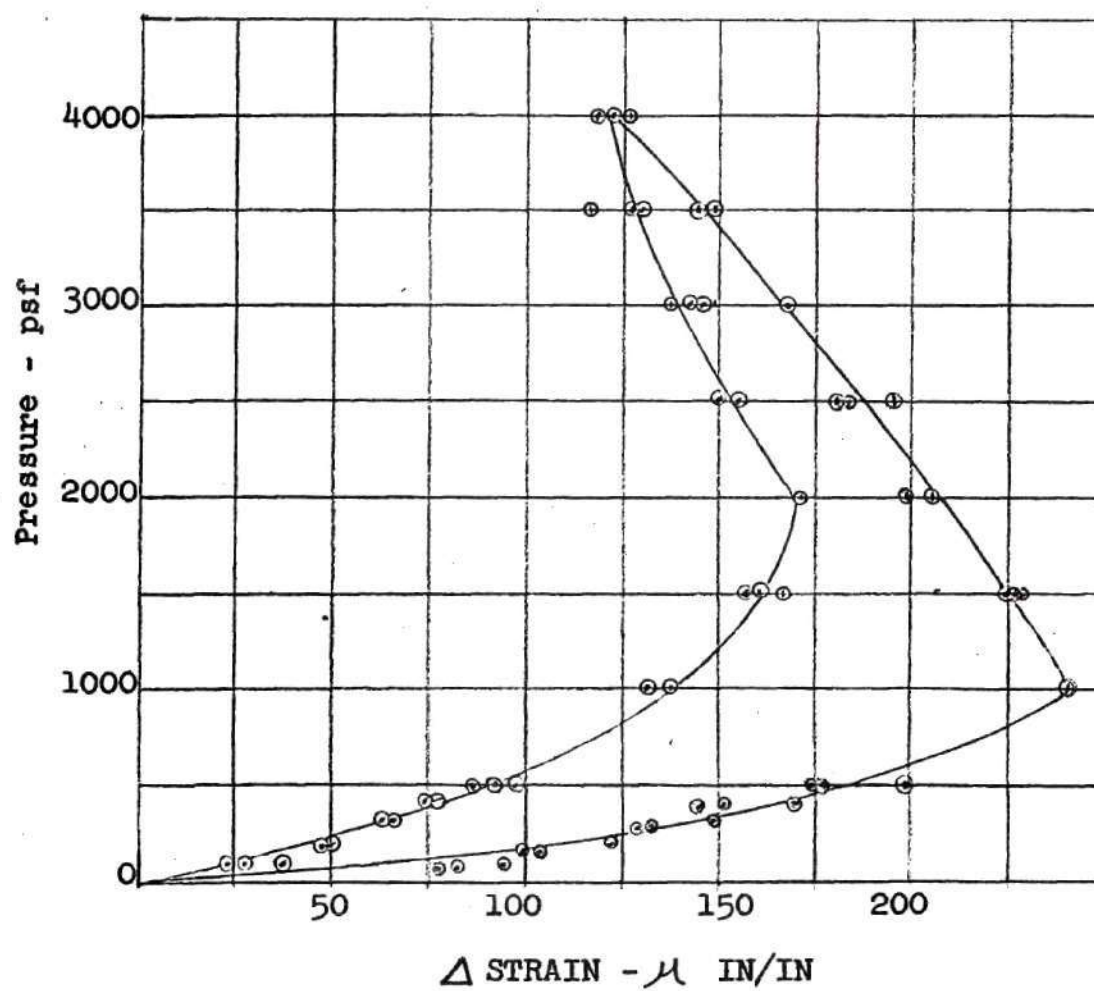


Fig. 20. Calibration Curve -  
Cell No. 2

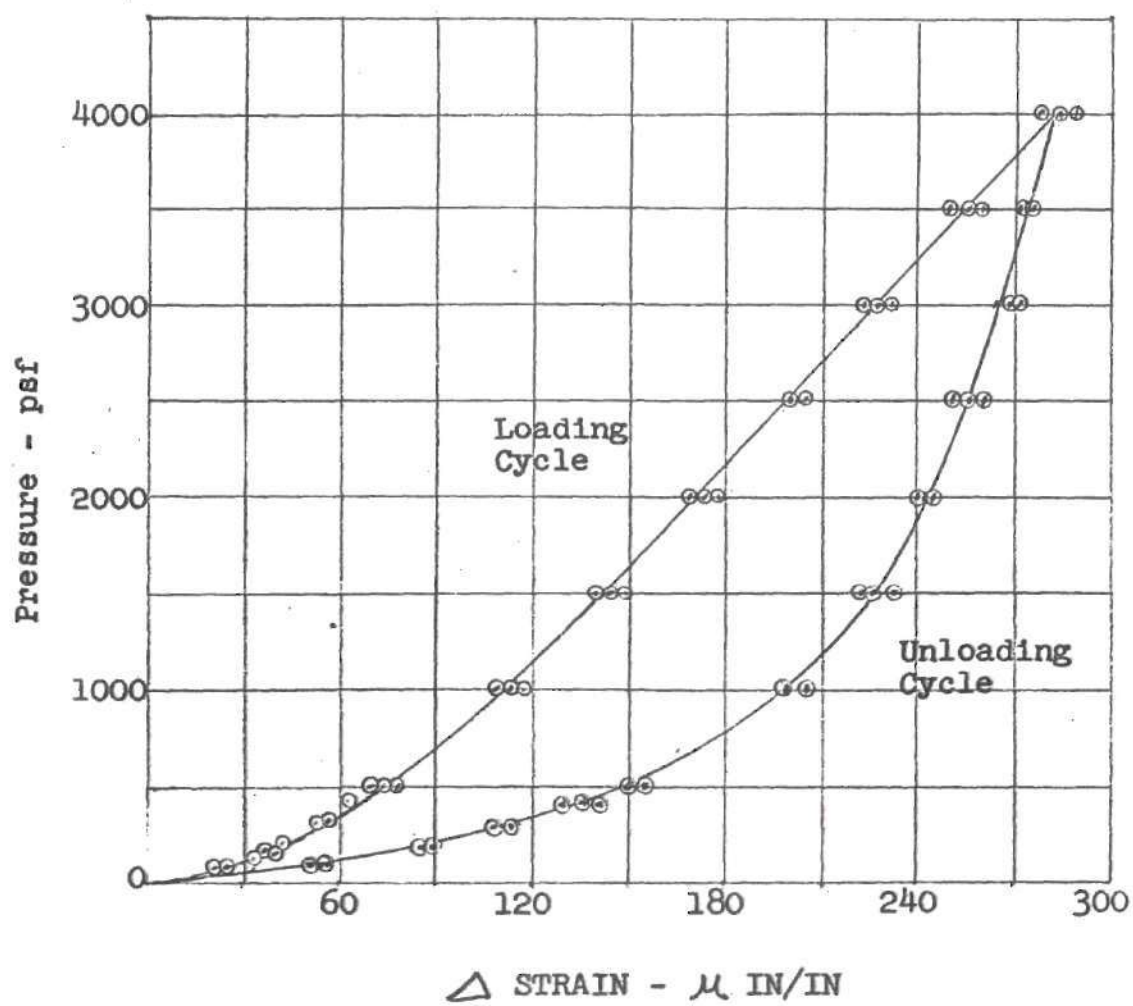


Fig. 21. Calibration Curve -  
Cell No. 3

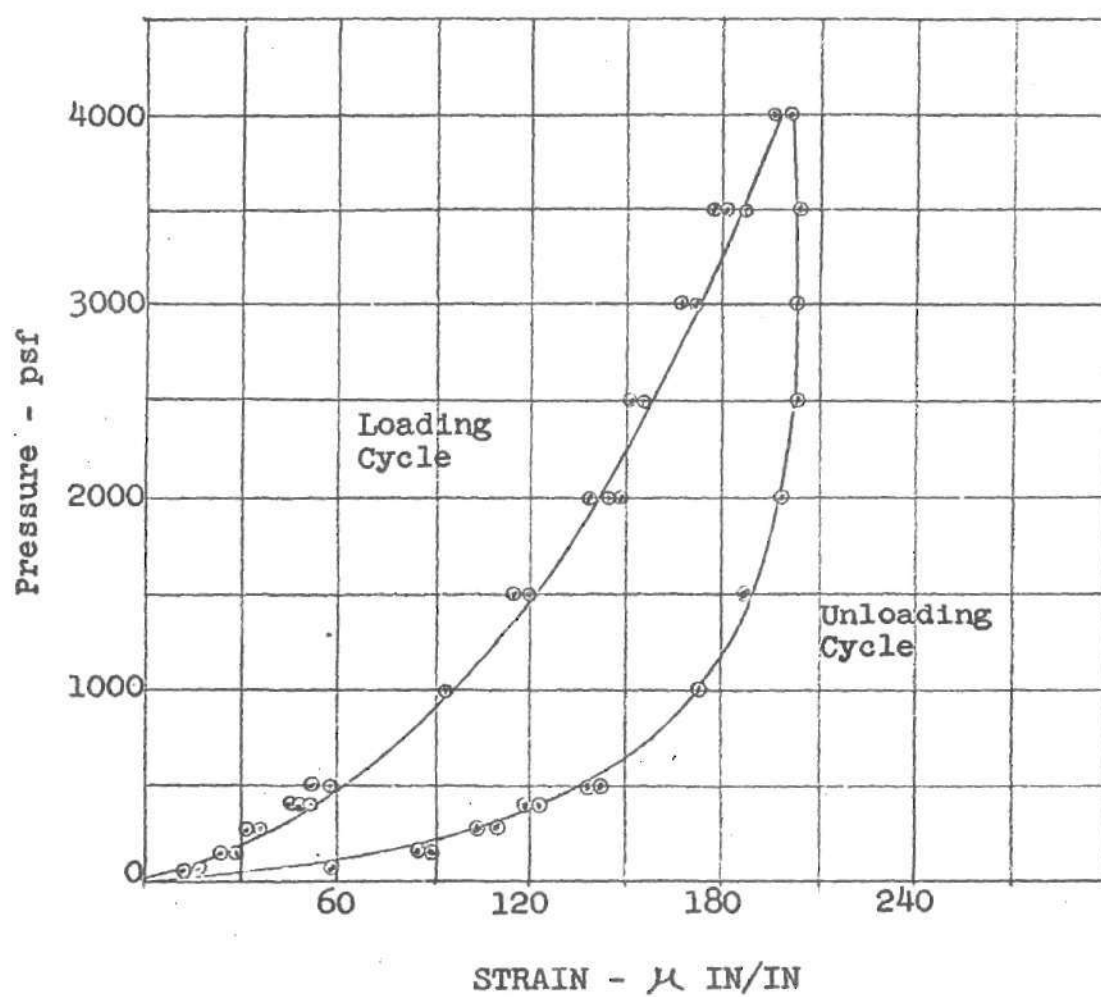


Fig. 22. Calibration Curve -  
Cell No. 4

Table 3. Test 1 - Dry-Tamped Soil

Time	Dial Reading - $\mu$ in/in					
	Top Cell		Middle Cell		Bottom Cell	
	Direct	Reverse	Direct	Reverse	Direct	Reverse
1350			11249	11260	11240	11239
1440			11249	11261	11263	11260
1455			11250	11263	11277	11210
1555	11223	11263	11262	11274	11299	11199
1730	11148	11133	11258	11274	11354	11148
1815	11148	11341	11268	11271	11358	11142
1915	11129	11348	11279	11250	11359	11140
2130	11132	11346	11280	11240	11343	11138
2220	11121	11346	11306	11222	11352	11141
0010	11129	11349	11302	11220	11348	11138
0050	11121	11349	11311	11220	11351	11149
0105	11125	11349	11309	11220	11348	11142
0205	11119	11343	11308	11217	11342	11149
0305	11122	11339	11306	11212	11333	11142
0415	11119	11339	11303	11214	11333	11152
0510	11123	11340	11308	11212	11333	11148
0620	11122	11337	11306	11214	11338	11149
0715	11122	11331	11302	11212	11334	11143
1115	11133	11313	11299	11203	11329	11151

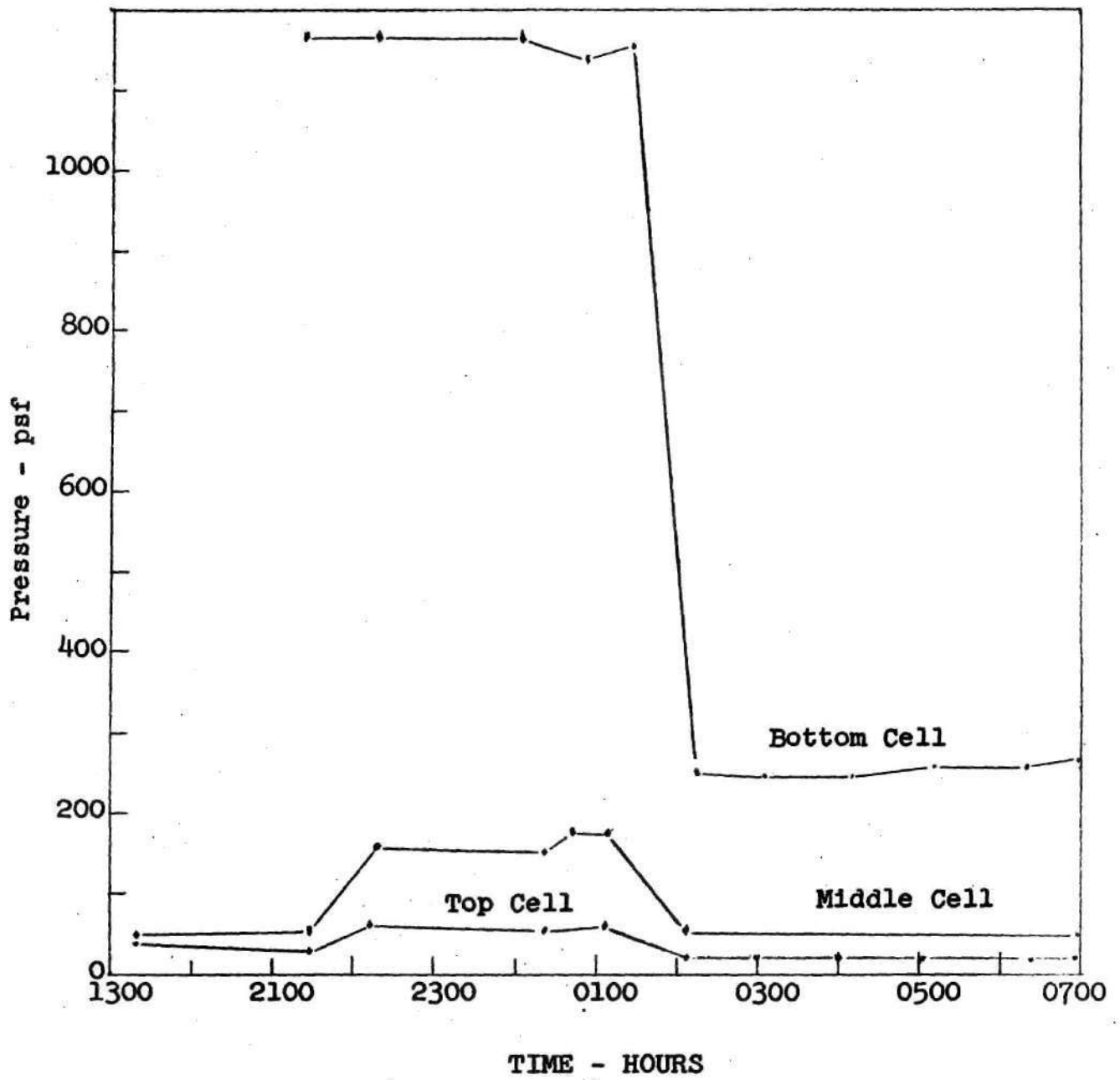


Fig. 23. Pressure-Time - Test No. 1



Table 4. Test 2 - Dry-Loose Soil

Time	Dial Reading - $\mu$ in/in					
	Top Cell		Middle Cell		Bottom Cell	
	Direct	Reverse	Direct	Reverse	Direct	Reverse
1730	11209	11249	11262	10830	11249	11219
1735	11201	11251	11262	11030	11252	11212
1740	11200	11253	11263	11056	11257	11213
1745	11206	11249	11270	11153	11262	11212
1800	11209	11259	11280	11153	11270	11213
1810	11227	11243	11272	11159	11277	11210
1825	11219	11254	11289	11160	11279	11217
1830	11221	11251	11283	11180	11280	11212
2040	11216	11242	11277	11134	11272	11206
2155	11219	11246	11281	11150	11276	11207
2240	11219	11249	11279	11159	11279	11209
2335	11225	11246	11279	11159	11279	11209
0105	11220	11235	11273	11089	11271	11199
0205	11215	11233	11270	11092	11270	11198

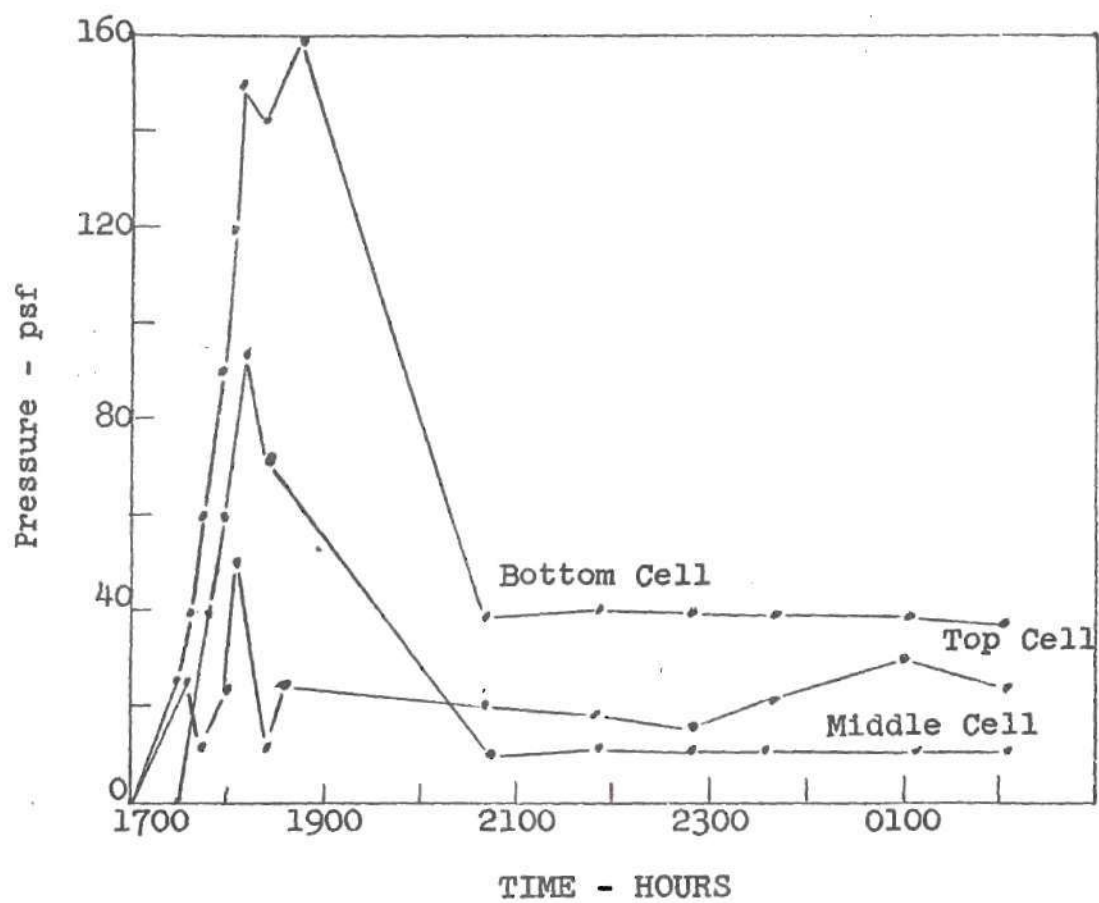


Fig. 24. Pressure-Time - Test No. 2

Table 5. Test 3 - Wet-Tamped Soil

Time	Dial Reading - $\mu$ in/in					
	Top Cell		Middle Cell		Bottom Cell	
	Direct	Reverse	Direct	Reverse	Direct	Reverse
1425	10999	11007	11002	11001	10999	10999
1445	11003	11008	11008	11001	11057	10923
1506	10999	11012	11012	11002	11088	10900
1518	10998	11018	11021	10998	11078	10918
1536	11042	10981	11039	10992	11050	10958
1600	11063	10963	11039	10999	11019	10988
1642	11068	10968	11048	10994	11010	11009
1721	11060	10960	11048	10988	11007	11000
1800	11060	10968	11050	10984	11000	11008
2030	11069	10952	11057	10970	10976	11030
2130	11062	10968	11068	10975	10962	11055
2230	11060	10963	11070	10970	10942	11072
2348	11062	10968	11078	10968	10922	11102
0030	11062	10966	11076	10962	10905	11108
0145	11058	10962	11077	10958	10880	11132
0230	11058	10962	11080	10958	10864	11158
0330	11054	10962	11080	10952	10846	11170
0406	11058	10960	11082	10954	10818	11208

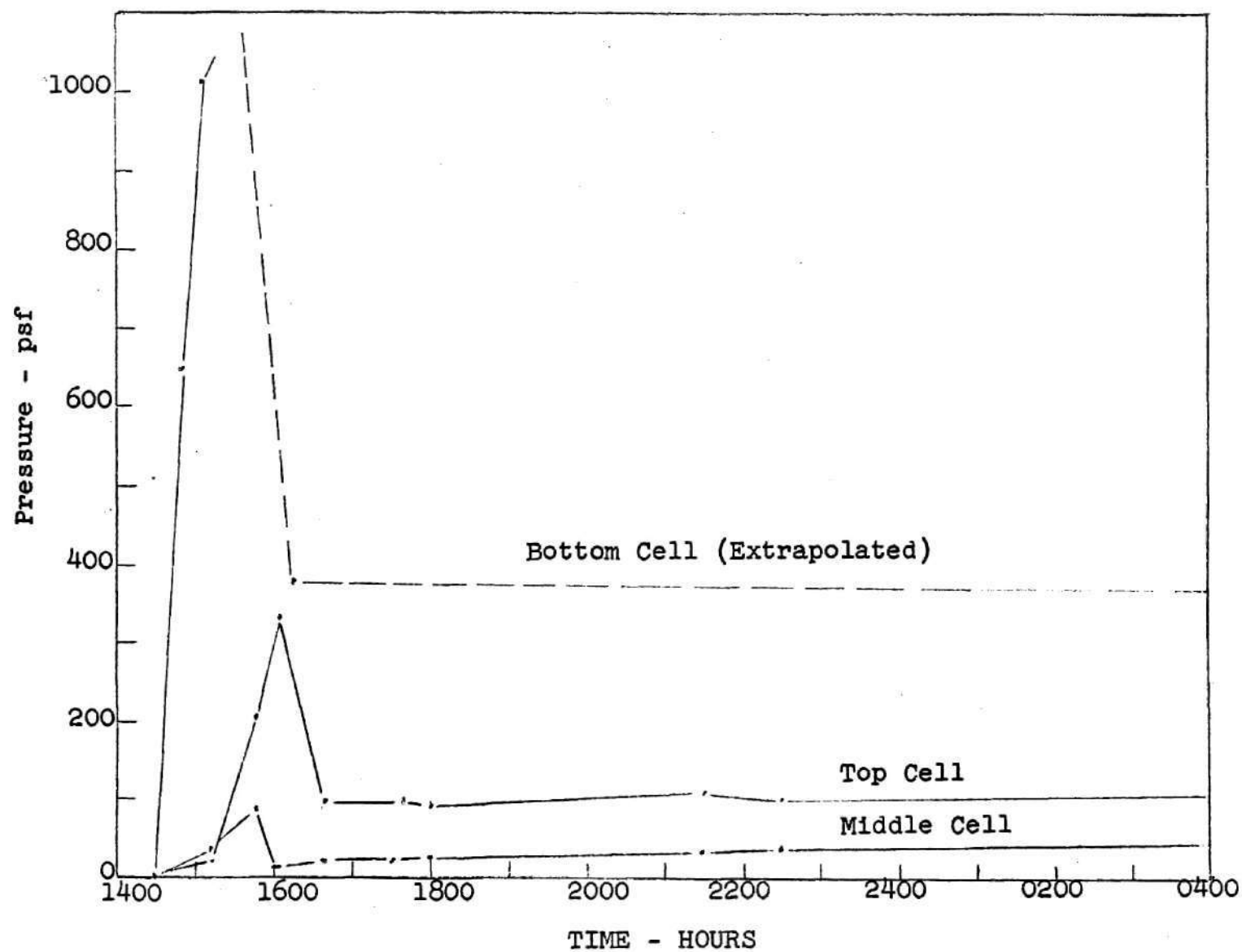


Fig. 25. Pressure-Time - Test No. 3

Table 6. Test 4 - Wet-Loose Soil

Time	Dial Reading - $\mu$ in/in					
	Top Cell		Middle Cell		Bottom Cell	
	Direct	Reverse	Direct	Reverse	Direct	Reverse
1218	11000	11000	11000	11000	11000	11000
1224	11008	11001	11002	11004	11007	11002
1242	11000	11022	11010	11012	11018	11009
1300	11018	11008	11011	11018	11021	11004
1318	11000	11023	11012	11016	11027	11009
1342	11027	11004	11017	11017	11029	11004
1400	11018	11018	11020	11018	11034	11008
1512	11028	11008	11021	11018	11034	11004
1712	11070	11068	11072	11064	11083	11053
2015	11052	11042	11058	11042	11072	11042
2154	11051	11051	11060	11044	11072	11043
2230	11112	11093	11112	11098	11130	11095
2306	11111	11114	11125	11111	11136	11111
2348	11098	11084	11099	11084	11114	11079
0030	11101	11101	11113	11094	11122	11091
0100	11139	11141	11149	11132	11159	11129

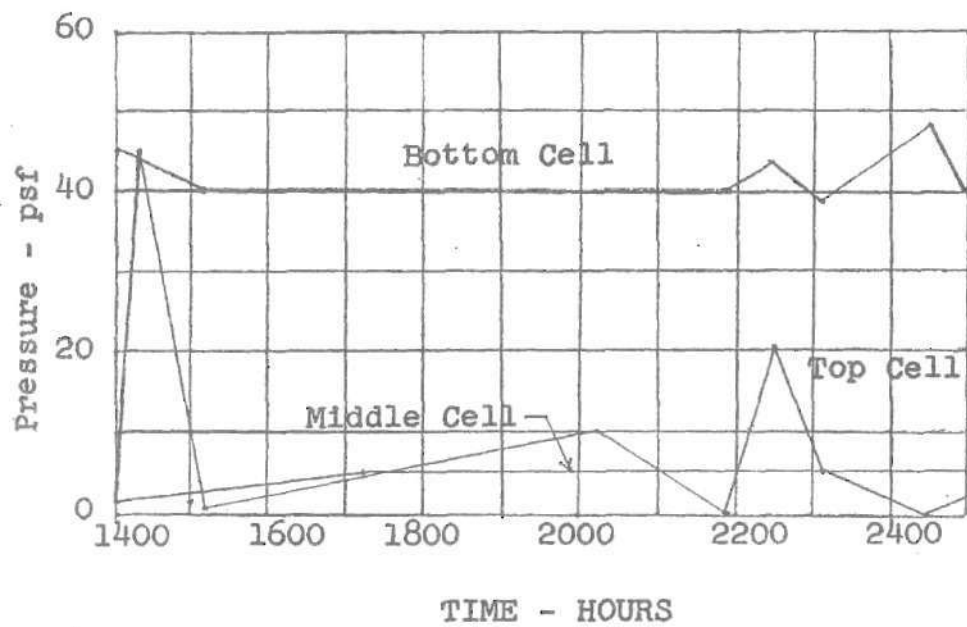


Fig. 26. Pressure-Time - Test No. 4



Table 7. Test 5 - Flooded Soil

Time	Dial Reading - $\mu$ in/in					
	Top Cell		Middle Cell		Bottom Cell	
	Direct	Reverse	Direct	Reverse	Direct	Reverse
1300	11000	11000	11000	11000	11000	11000
1330	11011	11000	11000	11010	11018	10993
1400	11005	11008	11002	11013	11030	10986
1430	11052	10972	11003	11027	11040	10990
1506	11031	10999	11008	11031	11053	10989
1530	11048	10982	11012	11028	11058	10988
1600	11030	10998	11012	11020	11050	10984
1630	11021	10988	11008	11016	11042	10984
1800	11020	11002	11010	11019	11039	10993
1830	11028	10988	11012	11013	11038	10992
2106	11019	10996	11010	11015	11025	11007
2206	11016	10992	11010	11000	11020	10998
2306	11022	10986	11014	11000	11022	10999
0006	11016	10999	11011	11001	11019	11003
0106	11022	10998	11020	11005	11028	11005
0206	11016	11000	11022	10998	11023	10999

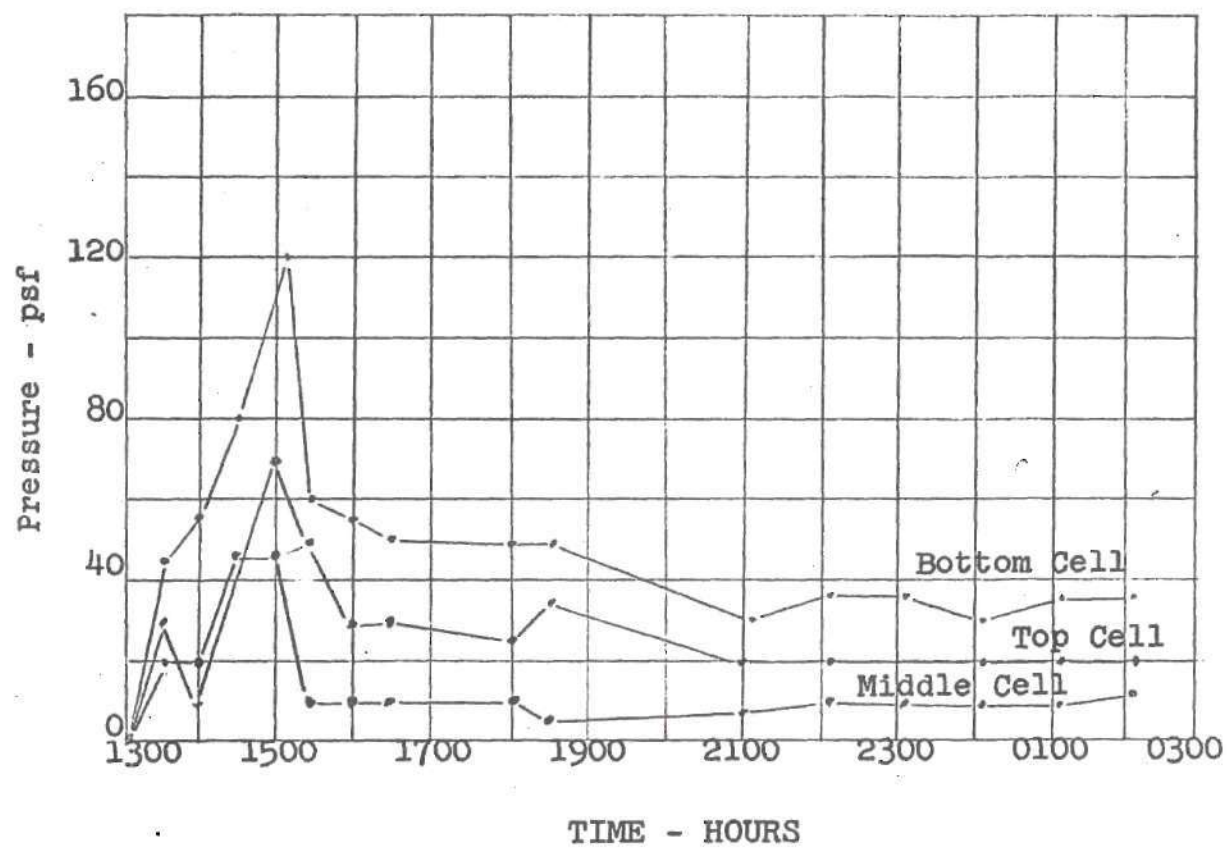


Fig. 27. Pressure-Time - Test No. 5

Table 8.    Average Water Content  
              And Average Density

Test	Average Water Content Percent	Unit Weight pcf
Dry-Tamped	3.8	93.0
Dry-Loose	3.5	78.0
Wet-Tamped	16.0	106.3
Wet-Loose	7.4	96.9
Flooded	36.5	107.2

## BIBLIOGRAPHY

## LITERATURE CITED

1. Coulomb, C. A., Essai sur une application des règles de maximis et minimis à quelques problèmes de statique relatifs à l'architecture, Mem. Div. Sav., Académie des Sciences, Paris, Vol. 7, 1776.
2. Goldbeck, A. T., "The Measurement of Earth Pressure on Retaining Walls," Proceedings Highway Research Board, Vol. II, 1938, pp. 66-80.
3. Mazanti, B. B., An Analysis of Foundations on Sand, Unpublished MS Thesis, Georgia Institute of Technology, 1955.
4. Perry, C. C. and H. R. Lissner, The Strain Gage Primer, New York, McGraw-Hill Book Company, Inc., 1955.
5. Rankine, W. J. M., "On the Stability of Loose Earth," Transactions, Royal Society, London, Vol. 147, 1857.
6. Robb, A. D., A Study of the Lateral Pressures Induced in a Soil Due to Compaction Under Confined Conditions, Unpublished MS Thesis, Georgia Institute of Technology, 1955.
7. Resál, J., La poussée des terres, Paris, 1910.
8. Spangler, M. G., "The Distribution of Normal Pressure on a Retaining Wall due to a Concentrated Surface Load," Proceedings of the First International Conference on Soil Mechanics, Vol. 1, 1936, pp. 200-207.
9. Spangler, M. G., "Horizontal Pressures on Retaining Walls Due to Concentrated Surface Loads," Iowa State Engineering Experiment Station, Bulletin 140, March, 1938.
10. Spangler, M. G., "Lateral Pressure on Retaining Walls Caused by Superimposed Loads," Proceedings Highway Research Board, Part II, 1938.
11. Terzaghi, K., "Old Earth Pressure Theories and New Test Results," Engineering News Record, Vol. 85, 1920.
12. Terzaghi, K., "A Fundamental Fallacy in Earth Pressure Computations," Journal, Boston Society of Civil Engineers, April, 1936.
13. Terzaghi, K., "Large Retaining Wall Tests," Engineering News Record, 1934, pp. 136, 259, 316, 403, 503.

14. Tschebotarioff, G. P. and J. D. Welch, "Effect of Boundary Conditions on Lateral Earth Pressures," Proceedings, Second International Conference on Soil Mechanics, 1948, Vol. 3, pp. 308,313.
15. Tschebotarioff, G. P., Soil Mechanics, Foundations and Earth Structures, New York, McGraw-Hill Book Company, Inc., 1948, p. 257.
16. Ibid, pp. 268-271.
17. Waterways Experiment Station, Corps of Engineers, U. S. Army, Vicksburg, Mississippi, "Pressure Cells for Field Use," Bulletin No. 40.



## OTHER REFERENCES

1. Baker, B., "The Actual Lateral Pressure of Earthwork," Proceedings, Institute of Civil Engineers, London, Vol. 65, Part 3, 1880-1881.
2. Benkelman, A. C. and R. J. Lancaster, " Important Considerations in the Design and Use of Pressure Cells," Proceedings, Highway Research Board, Vol. 20, 1941, pp. 299 ff.
3. Feld, J., "Review of Pioneer Work in Earth Pressure Determination and Recommendations for Earth Pressure Evaluation," Proceedings, Highway Research Board, 1940, pp. 730-749.
4. Goldbeck, A. T., "Soil Pressure Cell Measures Accurately to 1/10 Pound," Public Roads, August, 1950.
5. Jenkin, C. F., "The Pressure on Retaining Walls," Proceedings, Institute of Civil Engineers, Vol. 234, Session 1931 - 1932.
6. Mindlin, R. D., "Discussion of the Distribution of Normal Pressure on a Retaining Wall Due to A Concentrated Surface Load," Proceedings, First International Conference on Soil Mechanics, Vol. 3, pp. 155-156.
7. Packshaw, S., "Earth Pressure on Flexible Walls," Proceedings, Second International Conference on Soil Mechanics, Vol. 2, pp. 86-90.